Synthesis of Au/SnO₂ core–shell structure nanoparticles by a microwave-assisted method and their optical properties

Yeon-Tae Yu [a,b,*], Prabir Dutta [b]

[a] Division of Advanced Materials Engineering, College of Engineering, Chonbuk National University, Jeonju 561-756, South Korea
[b] Department of Chemistry, Ohio State University, Columbus, OH 43210, USA

ABSTRACT

Au/SnO₂ core–shell structure nanoparticles were synthesized using the microwave hydrothermal method. The optical and morphological properties of these particles were examined and compared with those obtained by the conventional hydrothermal method. In microwave preparation, the peak position of the UV–visible plasmon absorption band of Au nanoparticles was red-shifted from 520 to 543 nm, due to the formation of an SnO₂ shell. An SnO₂ shell formation was complete within 5 min. The thickness of the SnO₂ shell was 10–12 nm, and the primary particle size of SnO₂ crystallites was 3–5 nm. For the core–shell particles prepared by a conventional hydrothermal method, the shell formed over the entire synthesis period and was not as crystalline as those produced, using the microwave method. The relationship between the morphological and spectroscopic properties and the crystallinity of the SnO₂ shell are discussed.

© 2010 Elsevier Inc. All rights reserved.

1. Introduction

Core–shell structure composite nanoparticles (NPs) have attracted considerable attention as a means to design novel structures that are different from their single component counterparts [1–9]. Core–shell particles can also be used to create stable nanoparticle thin films [2,3]. The intrinsic optical and crystal structural characteristics of core–shell structure NPs can be maintained at high temperatures, because coalescence of the core material and crystal growth of the shell materials are greatly restricted [7]. Therefore, these core–shell composite nanoparticles have potential applications in optical processing, advanced coatings, photocatalysis and gas sensing.

Tin oxide (SnO₂), an n-type semiconductor with a wide band gap ($E_g = 3.62$ eV), is a key functional material that has attracted interest as a candidate for optoelectronic devices [10], gas sensors [11,12], transparent conducting electrodes [13,14] and catalyst supports [15]. The structural and physical properties, such as particle size and morphology, and crystallinity of these oxides depend on the synthesis route. The chemical and physical properties of Au/SnO₂ NP can also be altered by the particle size, morphology, crystal structure and crystallinity of the core and shell. Au/SnO₂ core–shell

nanoparticles were synthesized by Oldfield et al. who modified the optical properties of Au nanoparticles and monitored the electron density change within the core Au nanoparticles [16]. They used a precipitation method for synthesis and obtained Au/SnO₂ core–shell nanoparticle from the hydrolysis of sodium stannate. The surface plasmon (SP) band in the UV–visible absorption spectrum of Au nanoparticles was red-shifted, because the refractive index of the SnO₂ shell is greater than that of water. However, they reported considerable nucleation of free tin dioxide particles.

Recently, microwave-assisted synthesis has emerged as a novel method for producing many materials. Heat is generated internally within the material, instead of originating from external sources. Microwave heating is a promising technology, whose applications to the synthesis of nano-sized materials have also been growing rapidly owing to its unique effects, such as rapid volumetric heating, increased reaction rate and shortened reaction time, as well as the enhanced reaction selectivity and energy savings [17,18].

In this study, a microwave-assisted hydrothermal method was developed to control the optical properties of Au/SnO₂ core–shell NPs and reduce the formation of free tin dioxide during the synthesis reaction of Au/SnO₂ core–shell NPs. The SP absorption band and the morphology of the Au/SnO₂ core–shell NPs synthesized by a microwave hydrothermal method were examined and compared with those of the Au/SnO₂ core–shell NPs prepared by a conventional hydrothermal method. In addition, the relationship between the intensity of the SP band for Au/SnO₂ NPs and the crystallinity of the SnO₂ shell is discussed.

* Corresponding author at: Division of Advanced Materials Engineering, College of Engineering, Chonbuk National University, Jeonju 561-756, South Korea.
Fax: +82 63 270 2305.
  E-mail address: yeontae@jbnu.ac.kr (Y.-T. Yu).

2. Experimental details

The Au/SnO$_2$ core–shell nanoparticles were synthesized by using a conventional hydrothermal method according to the procedure reported elsewhere [16]. Details of a typical experiment are as follows. A HAuCl$_4$ solution (500 ml, 1 mM) was heated with mild stirring until boiling. A solution of tri-sodium citrate (25 ml, 34 mM) was then added with rapid stirring. The resulting solution was kept at 97 °C for 15 min with constant stirring, and allowed to cool. To coat the gold particles, the pH of the Au colloid solution (20 ml, 1 mM) was adjusted to 10.5 with sodium hydroxide (0.1 M). Sodium stannate (1 ml, 40 mM) was then added and the solution was stirred for 5 min. In the conventional hydrothermal method, the solution was heated to 60 °C for 10 min in a water bath and then maintained at 60 °C with rapid stirring for 2 h. In the microwave hydrothermal method, the solution was placed in a microwave oven (CEM Mars 5) and heated until the reaction temperature was reached (5 min), and was then maintained at that temperature with rapid stirring for 1 h. The reaction temperature in the microwave reaction ranged 100–180 °C. All chemical reagents in this study (purchased from the Aldrich Company, USA) were of analytical grade and used as received.

The ultraviolet visible absorption spectra were taken by a UV–visible spectrometer (UV-2550, Shimadzu). For the UV–visible spectra, the Au and Au/SnO$_2$ colloid was diluted to a final gold concentration of 0.167 mM. The transmission electron microscopy (TEM) images were taken on a Tecnai G2 FEI instrument at an accelerating voltage of 120 kV. The crystallographic structures of the solid samples were determined using a Rigaku Geigerflex X-ray diffractometer equipped with graphite monochromatized Cu-$K\alpha$ ($\lambda = 1.5405$ Å) radiation. The Raman spectra were recorded on a Renishaw^{TM} in Via Raman Microscope using a 633 nm argon ion laser excitation source and a 50 × objective.

3. Results and discussion

Fig. 1 shows the UV–visible absorption spectra of the Au/SnO$_2$ nanoparticle solutions during the deposition process of tin dioxide
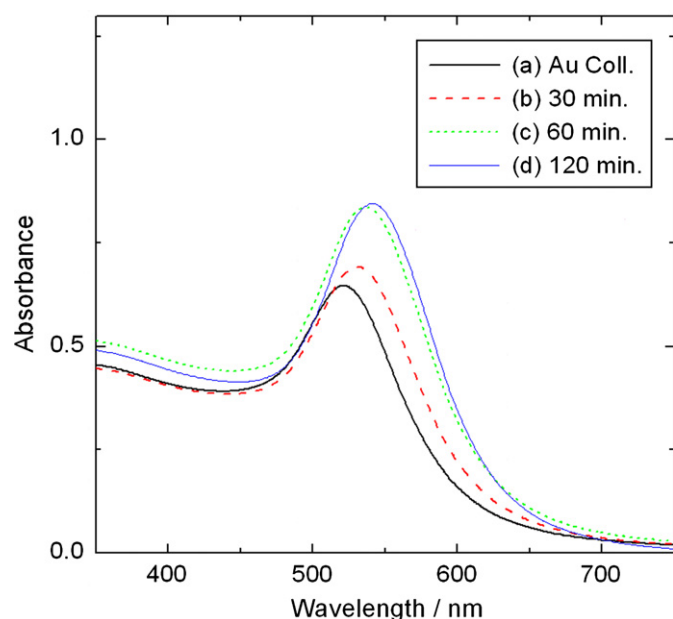
by a conventional hydrothermal method. The surface plasmon (SP) band of the Au nanoparticles red-shifted from 520 to 531 nm after a 30 min reaction time and then to 541 nm as the reaction time was extended to 120 min. The solution changed from a ruby red to an intense purple color.

Fig. 2 shows the UV–visible absorption spectra of the Au nanoparticle colloid during the deposition of an SnO$_2$ by the microwave hydrothermal method. In this experiment, the reaction temperature in the microwave oven was maintained at 120 °C, which was reached in 5 min. The SP band of the Au colloid shifted from 520 to 542 nm in the first 5 min of the reaction at 120 °C. The absorbance of the SP band increased gradually during the subsequent 55 min of reaction. The effect of temperature in the microwave method was examined at temperatures ranging 100–180 °C, keeping the reaction time at 1 h in all cases. Fig. 3 shows that the main effect of temperature is a slight increase in intensity and a blue shift.

The structural and morphological properties of the core–shell particles prepared by the two methods were examined. The morphology of the Au/SnO$_2$ core–shell structure nanoparticles synthesized by both conventional and microwave methods was examined by TEM (Fig. 4). Fig. 4a shows a TEM image of the Au/SnO$_2$ nanoparticles synthesized by the conventional method at 60 °C with a reaction time of 60 min, and Fig. 4b shows a TEM image of Au/SnO$_2$ nanoparticles synthesized by a microwave method at a reaction temperature of 120 °C, also with a reaction time of 60 min. Fig. 4c and d shows negative images of Fig. 4a and b, respectively, which provides a more precise view of the shape and size of SnO$_2$ nanoparticles in the shell layer. The core Au particle is 15 nm in diameter, and resultant core–shell structure of the Au/SnO$_2$ nanoparticles synthesized by both methods is clearly observed in these images. The thickness of an SnO$_2$ shell is also similar in both cases (10–12 nm). However, the particle size of SnO$_2$ in the shell layer using the conventional method was 1–2 nm, whereas it was 3–5 nm, using the microwave method.

Fig. 5 shows the electron diffraction patterns of Au/SnO$_2$ core–shell structure nanoparticles synthesized by a normal precipitation method and microwave hydrothermal method. The ring patterns of SnO$_2$ nanoparticles deposited on Au nanoparticles by the
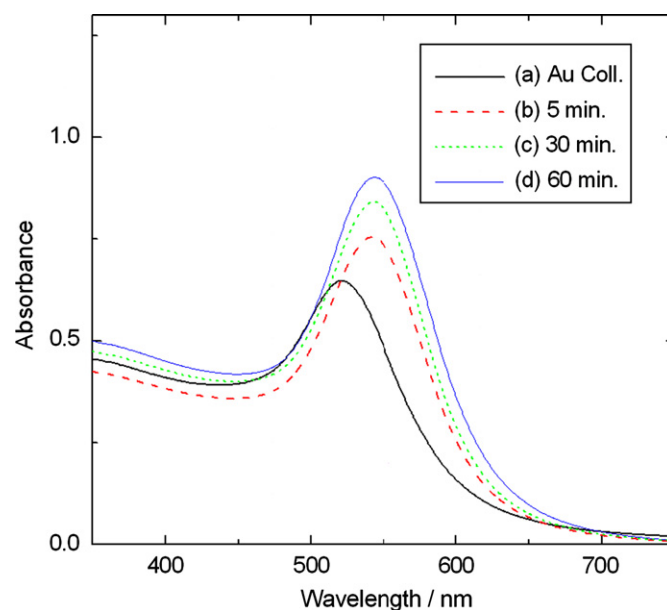

Fig. 1. UV–vis absorption spectra of the Au colloid and Au/SnO$_2$ core–shell NPs colloids synthesized by the hydrothermal method as a function of the reaction time at a reaction temperature of 60 °C.

Fig. 2. UV–vis absorption spectra of the Au colloid and Au/SnO$_2$ core–shell NPs colloids synthesized by the microwave hydrothermal method as a function of the reaction time at 120 °C.

microwave method were brighter than that of the particles prepared by the conventional method. This suggests that the SnO_2 shell formed on the Au core nanoparticles by the microwave method has better crystallinity.

Fig. 6 presents the X-ray diffraction patterns of the Au/SnO_2 core–shell structure nanoparticles synthesized by the
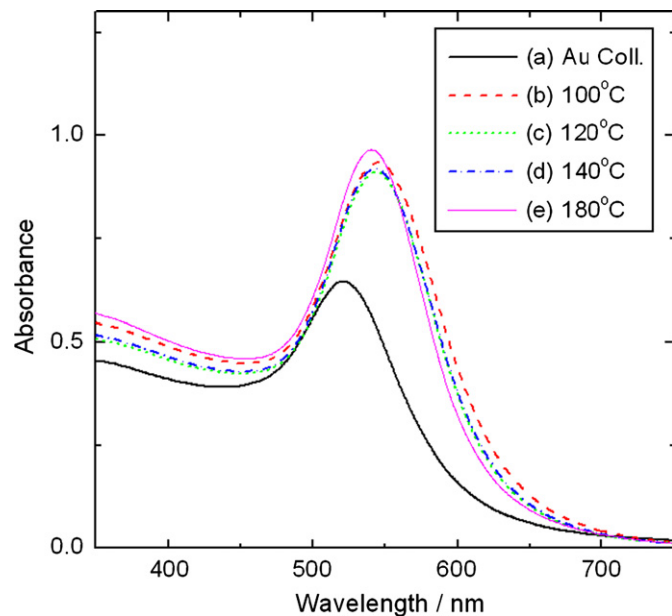

Fig. 3. UV–vis absorption spectra of the Au colloid and Au/SnO_2 core–shell NPs colloids synthesized by the microwave hydrothermal method as a function of the reaction temperature, all recorded after 60 min of reaction.

hydrothermal method and the microwave method at 100, 120, 140 and 180 °C. The crystal structure of the SnO_2 coated on the Au nanoparticles is consistent with cassiterite (JCPDS card no.: 41-1445) for all samples. There was a slight sharpening of the bands for the 180 °C microwave synthesis.

Raman spectrum analysis was carried out for the Au/SnO_2 samples prepared at 60 °C, using the conventional method and 140 and 180 °C by the microwave method. It is difficult to distinguish any peaks for the sample made by the hydrothermal method (Fig. 7a), whereas the microwave method led to samples
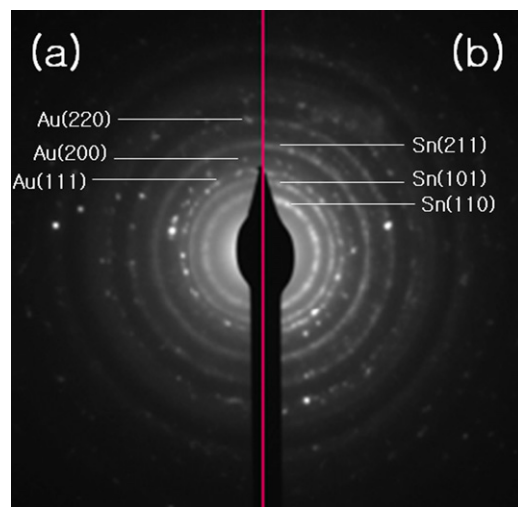

Fig. 5. Electron diffraction patterns of the Au/SnO_2 core–shell structure NPs synthesized by the conventional hydrothermal method (a) and the microwave hydrothermal method (b).
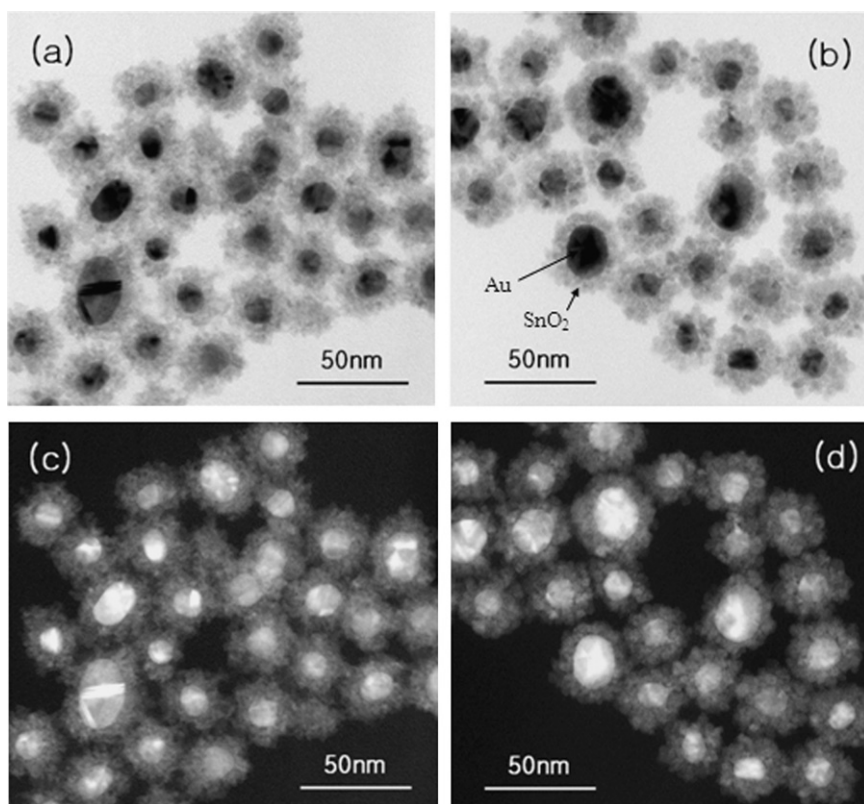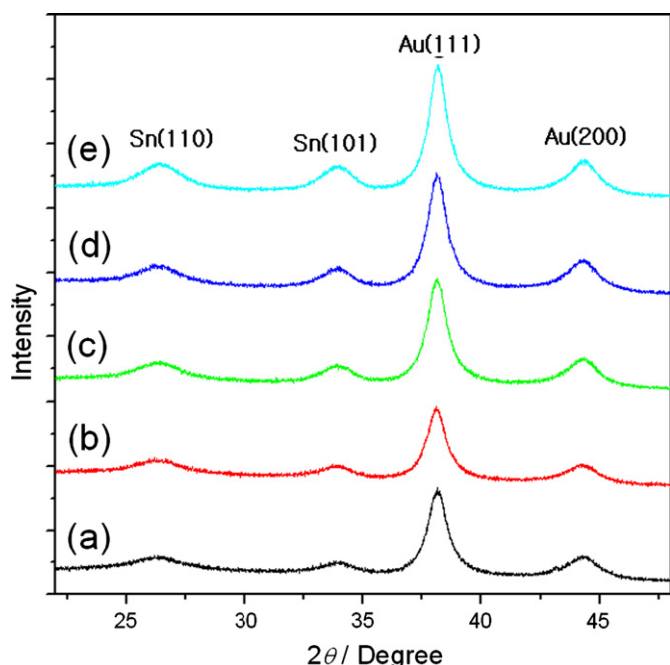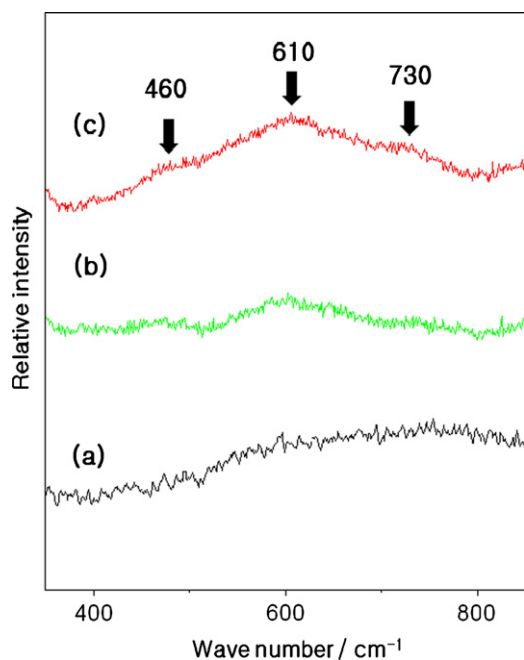

Fig. 4. TEM images of the Au/SnO_2 core–shell structure NPs synthesized by the conventional hydrothermal method (a, c) and microwave hydrothermal method (c, d). Photos (c) and (d) are negative images.

Fig. 6. X-ray diffraction patterns of the Au/SnO$_2$ core–shell NPs synthesized by the conventional hydrothermal method (a) and the microwave hydrothermal method (b–e) at reaction temperatures of (a) 60 °C, (b) 100 °C, (c) 120 °C, (d) 140 °C and (e) 180 °C.

Fig. 7. Raman spectra of the Au/SnO$_2$ core–shell NPs synthesized by the conventional hydrothermal method at 60 °C (a) and microwave hydrothermal method at (b) 140 °C and (c) 180 °C.

with peaks at 460, 610 and 730 cm^{-1}. Previous studies reported that the peaks of crystalline SnO$_2$ occur at 472, 630 and 773 cm^{-1} [19–21]. The decrease in the frequencies for the core–shell particles could arise from their nanocrystalline nature [22].

The Raman spectra, TEM images and XRD patterns show that the SnO$_2$ shell synthesized by the microwave method is composed of SnO$_2$ particles with a larger particle size and higher crystallinity than the SnO$_2$ shell prepared by the conventional method.
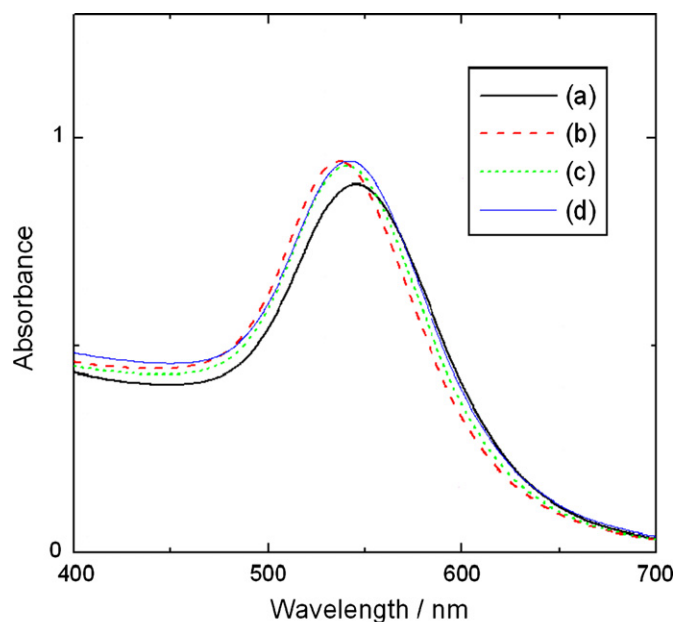
Fig. 8. UV–vis absorption spectra of the Au/SnO$_2$ core–shell NPs colloids synthesized by the microwave hydrothermal method after UV irradiation (254 nm): (a) Au/SnO$_2$ NPs colloid synthesized at 180 °C, (b) after UV irradiation for 1 h, (c) 1 h after UV light off, and (d) 1 day after UV light off.

The optical spectra shown in Figs. 1 and 2 suggest that red-shift of the Au SP bands is due to the shell layer. Oldfield et al. attributed this red-shift to the higher refractive index of the SnO$_2$ shell compared to water [16]. Based on the time dependence of the red-shifts observed in Figs. 1 and 2, it appears that in the case of the microwave method, the shell is formed within the first 5 min of synthesis, whereas shell formation extended over the entire synthesis time in the hydrothermal method. From the structural and morphological data, the increase in the SP band intensity of Au/SnO$_2$ in Figs. 1 and 2 originated from the increase in crystallinity of SnO$_2$ particles.

Fig. 8 shows the effect of UV irradiation on the peak position of the SP band of the Au/SnO$_2$ core–shell nanoparticles prepared by the microwave method. The peak position was blue-shifted from 543 to 537 nm upon irradiation with 254 nm for 1 h. This suggests that the electrons, produced from the valence band of the SnO$_2$ shell by UV irradiation, accumulate on the surface of the Au core nanoparticles, due to the lower Fermi level of the Au nanoparticles compared to the conduction band of an SnO$_2$. In other words, the Au core nanoparticles act as an electron collector in the Au/SnO$_2$ core–shell system with UV light. The SP band showed a red-shift after removing the UV irradiation, but the process was slow on the time scale of hours. From this result, it is expected that Au/SnO$_2$ core–shell nanoparticles should find applications as photocatalysts, nano-capacitors, optoelectronics and sensor materials.

4. Conclusion

Au/SnO$_2$ core–shell structure nanoparticles were successfully synthesized by the microwave hydrothermal process. The thickness of the SnO$_2$ shell was 10–12 nm, and the primary particle size of an SnO$_2$ was 3–5 nm. The formation time of the SnO$_2$ shell on the surface of the Au nanoparticles was faster than that with the conventional hydrothermal method. In the microwave synthesis, the SnO$_2$ shell was formed within 5 min, and the peak position of the SP absorption band of the Au nanoparticles was red-shifted from 520 to 543 nm, due to the formation of an SnO$_2$ shell. The

increasing intensity of the SP band of Au/SnO_2 core–shell nanoparticles during the microwave reaction was attributed to an increase in the crystallinity of the SnO_2 shell. The SP band of the Au/SnO_2 core–shell nanoparticles was blue-shifted upon UV irradiation, because the electrons produced from the valence band of an SnO_2 accumulated on the surface of the Au nanoparticles.

Acknowledgments

References

[1] F. Caruso, Adv. Mater. 13 (2001) 11.
[2] T. Ung, L.M. Liz-Marzan, P. Mulvaney, Langmuir 14 (1998) 3740–3748.
[3] T. Ung, L.M. Liz-Marzan, P. Mulvaney, J. Phys. Chem. B 105 (2001) 3441–3452.
[4] Y.D. Yin, Y. Lu, Y.G. Sun, Y.N. Xia, Nano Lett. 2 (2002) 427–430.
[5] X. Wang, Q. Peng, Y.D. Li, Acc. Chem. Res. 40 (2007) 635–643.
[6] H.W. Kwon, Y.M. Lim, S.K. Tripathy, B.G. Kim, M.S. Lee, Y.T. Yu, Jpn. Appl. Phys. 46 (2007) 2567–2570.
[7] S.K. Tripathy, H.W. Kwon, Y.M. Leem, B.G. Kim, Y.T. Yu, Chem. Phys. Lett. 442 (2007) 101–104.
[8] H. Song, Y.M. Leem, B.G. Kim, Y.T. Yu, Mater. Sci. Eng. B 143 (2007) 70–75.
[9] X. Wu, H. Song, J.M. Yoon, Y.T. Yu, Y.F. Chen, Langmuir 25 (2009) 6438–6447.
[10] J.S. Lee, S.K. Sim, B. Min, K. Cho, S.W. Kim, S. Kim, J.Cryst. Growth 267 (2004) 145–149.
[11] G. Faglia, C. Baratto, G. Sberveglieri, Appl. Phys. Lett. 85 (2005) 11923.
[12] G. Xu, Y.W. Zhang, X. Sun, C.L. Xu, C.H. Yan, J. Phys. Chem. B 109 (2005) 3269–3278.
[13] Y. Wang, J.Y. Lee, J. Phys. Chem. B 108 (2004) 17832–17837.
[14] H. Sugimoto, H. Tsukube, K. Tanaka, Eur. J. Inorg. Chem. 23 (2004) 4550–4553.
[15] N.Q. Jia, Q. Zhou, L. Liu, M.M. Yan, Z.Y. Jiang, J. Electroanal. Chem. 580 (2005) 213–221.
[16] G. Oldfield, T. Ung, P. Mulvaney, Adv. Mater. 12 (2000) 1520–1522.
[17] V. Subramanian, W. Burke, H. Zhu, B.J. Wei, Phys. Chem. C 112 (2008) 4550–4556.
[18] A. Srivastava, S.T. Lakshmikumar, A.K. Srivastava, K. Jain, Sensors Actuators B 126 (2007) 583–587.
[19] L. Abello, B. Bochu, A. Gaskov, S. Koudryavtseva, G. Lucazeau, M.J. Roumyantseva, Solid State Chem. 135 (1998) 78–85.
[20] M. Ristic, M. Ivande, S. Popovic, S.J. Music, Non-Cryst. Solids 303 (2002) 270–280.
[21] A. Cabot, A. Dieguez, A. Romano-Rodriguez, J.R. Morante, N. Barsan, Sensors Actuators B 79 (2001) 98–106.
[22] A. Dieguez, A. Romano-Rodriguez, A. Vila, J.R. Morante, J. Appl. Phys. 90 (2001) 1550–1557.